DEPARTMENT OF THE INTERIOR

U.S. GEOLOGICAL SURVEY

Two-dimensional finite element models of the variation of heat flow with depth caused by refraction at a low conductivity graben

by

R.W. Saltus and A.H. Lachenbruch

Open-File Report 87-618

Menlo Park, California
1987

Abstract

The variation of vertical heat flow with depth near a scarp juxtaposing two media of contrasting thermal conductivity is summarized in a series of plots. Heat flows are calculated numerically using a two-dimensional finite element model. Boundary conditions are: uniform, constant temperature at the Earth's surface; constant heat flux into the bottom of the model (at great depth); no horizontal heat flow across the sides of the model; temperature and the normal component of heat flow are continuous across the conductivity boundaries. For geologically extreme (but plausible) conductivity variations this refraction effect may cause heat flow to vary from 40% to 200% of the regional value. In general, the refraction effect is felt to within several scarp heights, both vertically and horizontally.

Introduction

When rocks of contrasting thermal conductivities are juxtaposed on steep contacts, heat flows preferentially through the rock with the higher conductivity. For example, if surface heat flow is measured on either side of a vertical fault separating granite from alluvium, the measured value will be higher over the more conductive granite. The maximum effect will occur at the contact itself, where the heat flow will vary discontinuously by an amount equal to the ratio of the thermal conductivities of the two rock types. This follows from Fourier's law of heat conduction:

$$q \equiv k\frac{\partial \Theta}{\partial z}$$

where:

q = vertical heat flow (W/m^2)

k = thermal conductivity ($W/m°K$)

Θ = temperature ($°K$)

z = vertical distance (m)

The vertical thermal gradient $\partial\Theta/\partial z$, is continuous because temperature, Θ, is continuous at the boundary. Thus $\partial\Theta_1/\partial z = \partial\Theta_2/\partial z$, and therefore, $q_1/q_2 = k_1/k_2$. The maximum contrast in vertical heat flow is the ratio of the thermal conductivities.

If the steep contact (scarp) is buried under a uniform surface cover, the heat flow at the surface will no longer be discontinuous over the contact. Similarly, if heat flow is measured in a uniformly conducting region below the contact, the perturbation is less intense and more diffuse with depth.

A previous analysis of heat flow variation caused by effects of contrasting thermal conductivity concentrated on the surface variation caused by a series of valleys with semi-elliptic cross section (Lachenbruch and Marshall, 1966). The analytic solution for the semi-elliptic case was supplemented by finite difference models for basins with rectangular cross section. This report extends the analysis by computing the heat flow at depth. Current acquisition of down-hole temperature measurements as a part of deep scientific drilling (DOSECC Investigators and Staff, 1987) has prompted this work.

The heat flows presented in figures 2-5 were calculated numerically using a 2-dimensional finite element program (VFINI2 by T. C. Lee, U. C. Riverside).

The models

Vertical heat flow curves are calculated at a series of depths through two classes of model: graben and step. Both model classes have zones of lower thermal conductivity with rectangular cross section. The graben has a ratio of half-width to height of 4, the step (approximated by a wide graben) has a ratio of 50. For each of these two classes, calculations were made for 3 different thermal conductivity contrasts (see table 1 and figures 2-4). A fourth set (figure 5) shows the heat flow variation for a graben and step that are buried under a low conductivity surface cover to a depth of 1/2 the scarp height.

The five parameters that describe the model geometry are illustrated in figure 1. The parameters are:

a = Depth of burial of the top of the scarp.

b = Height of the graben-bounding scarp.

c = Half-width of the graben.

X = Total width of the finite element model.

Z = Total height of the finite element model.

In table 1 these parameters are normalized by the step height, b. The final parameter that characterizes the model is the normalized contrast in thermal conductivity:

$$\Delta k = \frac{k_1 - k_2}{k_1} = 1 - \frac{k_2}{k_1}$$

where k_1 is the basement thermal conductivity and k_2 is the (lower) thermal conductivity of the graben fill.

Table 1: Model parameters (see figure 1 for a diagram of the model geometry).

figure	*name*	a/b	c/b	X/b	Z/b	Δk
2	graben	0	4	50	20	0.2
	step		50	100		
3	graben	0	4	50	20	0.4
	step		50	100		
4	graben	0	4	50	20	0.8
	step		50	100		
5	buried graben	0.5	4	50	20.5	0.4
	buried step		50	100		

The finite element method

The differential equation of steady-state conduction of heat in an isotropic solid is given by Laplace's equation (Carslaw and Jaeger, 1959, p. 9, eq. 6):

$$\nabla^2\Theta = 0$$

or, in two dimensions, for two media of contrasting conductivity:

$$\frac{\partial^2\Theta_1}{\partial x^2} + \frac{\partial^2\Theta_1}{\partial z^2} = 0$$

in medium one, and

$$\frac{\partial^2\Theta_2}{\partial x^2} + \frac{\partial^2\Theta_2}{\partial z^2} = 0$$

in medium two, where Θ is temperature.

For the solution obtained here, the following boundary conditions are assumed:

1. Uniform, constant temperature at the Earth's surface.
2. Constant heat flux across the bottom surface of the model (at depth Z).
3. The horizontal temperature gradient is required to be zero at the sides of the model. This condition creates a "mirror" image of the model geometry at each side.
4. Continuity of normal flux ($k_1\partial\Theta_1/\partial n = k_2\partial\Theta_2/\partial n$) and temperature across the boundary between medium one and medium two.

In the finite element method, the physical continuum is approximated by discrete elements (see Desai and Abel, 1972, for a complete treatment of the method). For the analysis in this report, the elements are rectangular, each with four corner nodes. The rows and columns of the element matrix have uneven spacing. Row elements are smaller near the surface and column elements are smaller near the scarp, to give greater accuracy where the heat flow varies the most. Figure 6 illustrates the node spacing for the graben and step models.

The solution to the steady-state heat flow problem is approximated by treating the heat balance at each element separately. The same conservation of energy principles that are the basis for Laplace's equation are instead interpreted for each element in terms of the temperatures at the adjacent nodes. A system of simultaneous linear equations is constructed from these node equations and constrained by the boundary conditions. This set of equations is solved for the temperature at each node. Vertical heat flow is then calculated by multiplying the vertical temperature gradient (approximated by the difference in temperature between two nodes adjacent vertically) by the local thermal conductivity.

Results

Figures 2-5 contain the results of this study. Each plot consists of a series of curves, each depicting normalized vertical heat flow as a function of distance from the graben-bounding scarp. Heat flow is normalized to the constant flow into the bottom of the model (boundary condition 2). The curves are labeled with their depths. All spatial dimensions are normalized to the scarp height, b.

Figure 2 contains the heat flow curves for a graben and step model with a small thermal conductivity contrast ($k_1/k_2 = 1.25$, or $\Delta k = 0.2$). This could apply to the case of granite against a low-porosity sandstone, for example. The maximum perturbation is about 10% of the regional heat flow. The graben and step cases are not significantly different near the scarp. Within 2 scarp heights horizontally, or one scarp height vertically, the refraction effect drops below 5% of the background.

Figure 3 contains the heat flow curves for a graben and step model with a moderate contrast in thermal conductivity ($k_1/k_2 = 1.67$, or $\Delta k = 0.4$). This could apply to the case of granite against high-porosity sandstone, for example. The maximum perturbation is about 25% of the regional heat flow. The graben and step cases do not differ significantly over the high conductivity (right) side of the model. Within 3 scarp heights horizontally or 1.5 vertically, the effect diminishes to below 5%, except in the center of the graben where the perturbation exceeds 5% to a depth of 4 scarp heights.

Figure 4 contains the heat flow curves for a graben and step model that juxtapose media with a large conductivity difference ($k_1/k_2 = 5$, or $\Delta k = 0.8$). This case could apply to granite against alluvium or to ice against snow, for example. Because the temperature gradients arising from the step case are greater than those for the graben case, the heat flow contrast across the step is larger. This is the case for the previously discussed models as well, although the effect is not as pronounced at the lower conductivity contrasts. Heat flow varies from less than 40% (the minimum for the graben model) to more than 200% (the maximum for the step model) of the regional value. The perturbation effect is still 10% at a distance of 5 scarp heights from the graben horizontally, or to a distance of 10 scarp heights from the step case. Within the center of the graben, the perturbation is still -20% to a depth of 4 scarp heights.

Figure 5 contains the heat flow curves for a buried graben and step of moderate conductivity contrast ($k_1/k_2 = 1.67$ or $\Delta k = 0.4$). The magnitude of the effect is the same as for the models depicted in figure 3, the matching unburied case. The surface heat flow (curve 0) is continuous, the discontinuity showing up from 0.5 to 1.5 scarp heights, the depth position of the scarp in the model. Since these calculation depths between the top and bottom of the scarp (0.5, 1, and 1.5) are farther from the isothermal surface boundary condition than their companion depths (0, 0.5, and 1) from the unburied case (figure 3), the heat flow perturbation falls off somewhat more quickly with horizontal distance near the scarp for this model as compared to the unburied model.

In conclusion, the heat flow perturbations caused by refraction at a steep conductivity contact may be a significant fraction of the true regional heat flow. Care must be taken in the extrapolation of surface heat flow measurements to depth. Consideration must be given to the local geology since the models in this report show that a low conductivity basin of great depth may effect the surface heat flow to considerable distance. The effects noted in this report should be easy to detect if heat flows are obtained in a network of enough horizontal density.

References

Carslaw, H. S., and Jaeger, J. C., **1959**, *Conduction of heat in solids*, Oxford University Press (second edition), Oxford, England

Desai, C. S., and Abel, J. F., **1972**, *Introduction to the finite element method - a numerical method for enginerering analysis*, Van Nostrand Reinhold Company, New York, N. Y.

DOSECC Investigators and Staff, **1987**, DOSECC continental scientific drilling program: *EOS Transactions, American Geophysical Union*, Vol. 68, No. 21, p. 545-546

Lachenbruch, A. H., and Marshall, B. V., **1966**, Heat Flow Through the Arctic Ocean Floor: The Canada Basin - Alpha Rise Boundary, *Journal of Geophysical Research*, v71, n4, p1223-1248

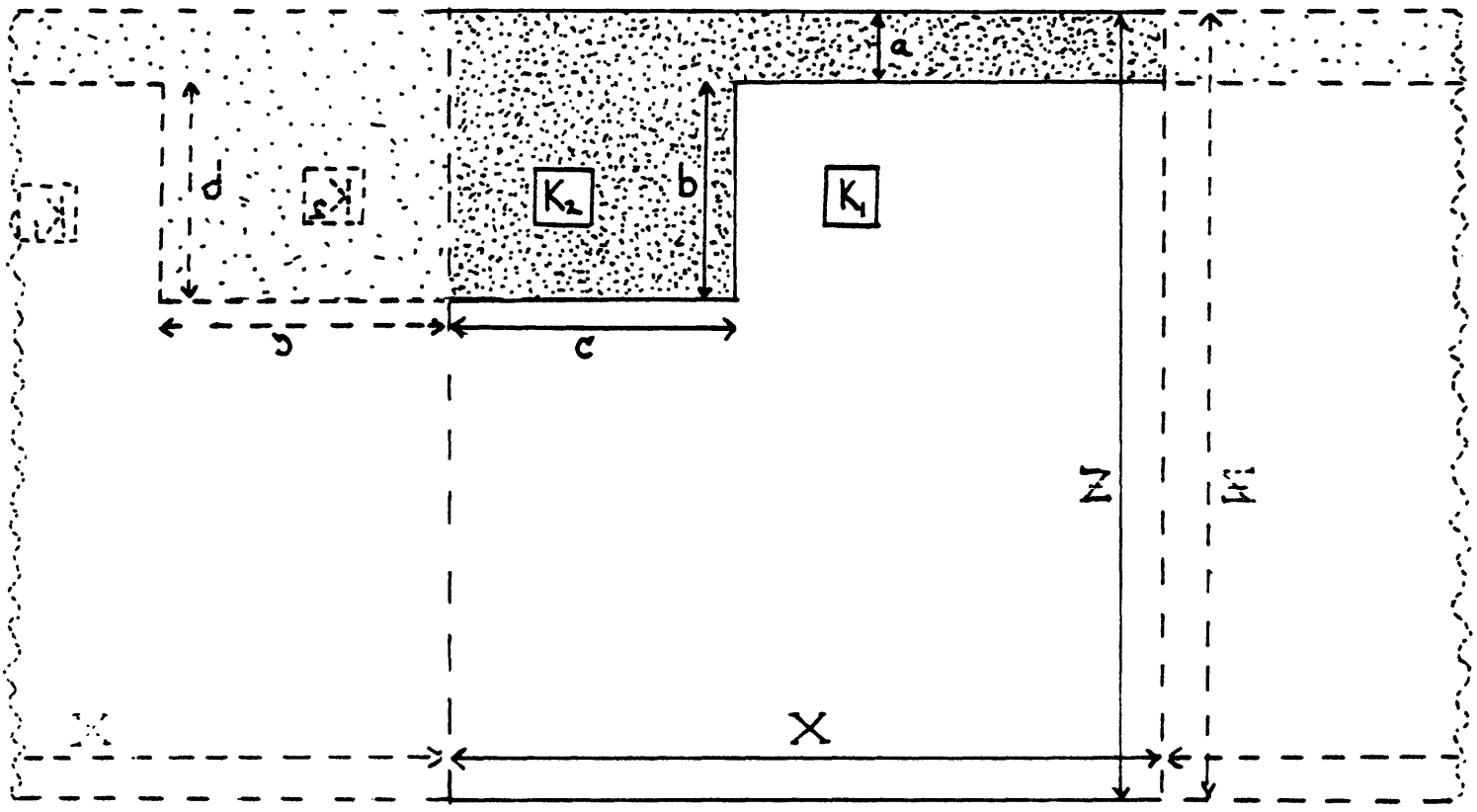

Figure 1: Geometry of the thermal conductivity model. All distances are normalized to the scarp height, b.

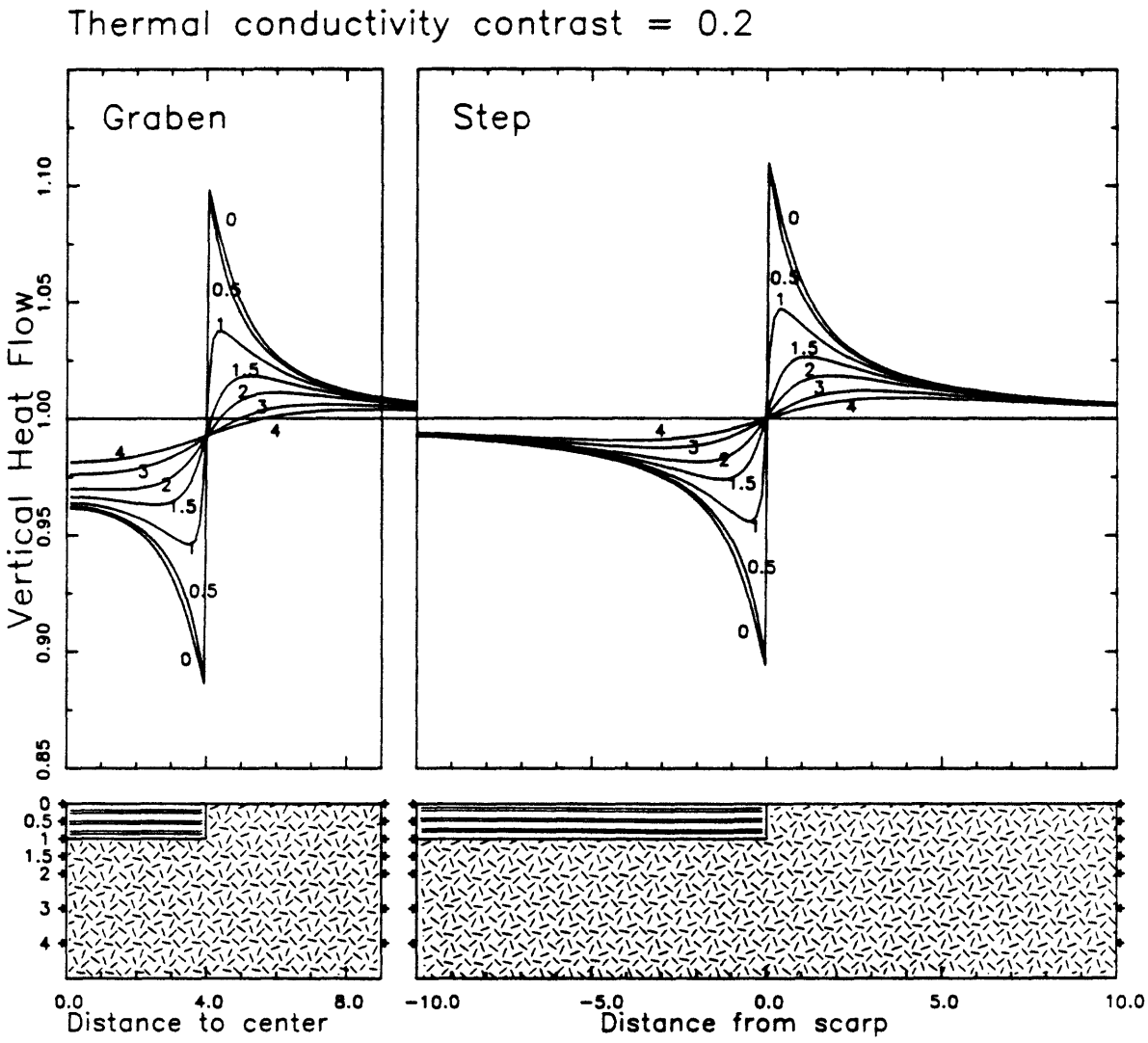

Figure 2: The variation of vertical heat flow with depth over two models juxtaposing material of small difference in thermal conductivity at a steep surface contact. Each heat flow curve is labeled with its calculation depth, normalized to scarp height. The lower blocks of the figure depict the model geometry. Small arrows mark the depths where heat flow is calculated. The stippled region has low thermal conductivity compared with the rest of the model. All distances are normalized to a unit scarp height.

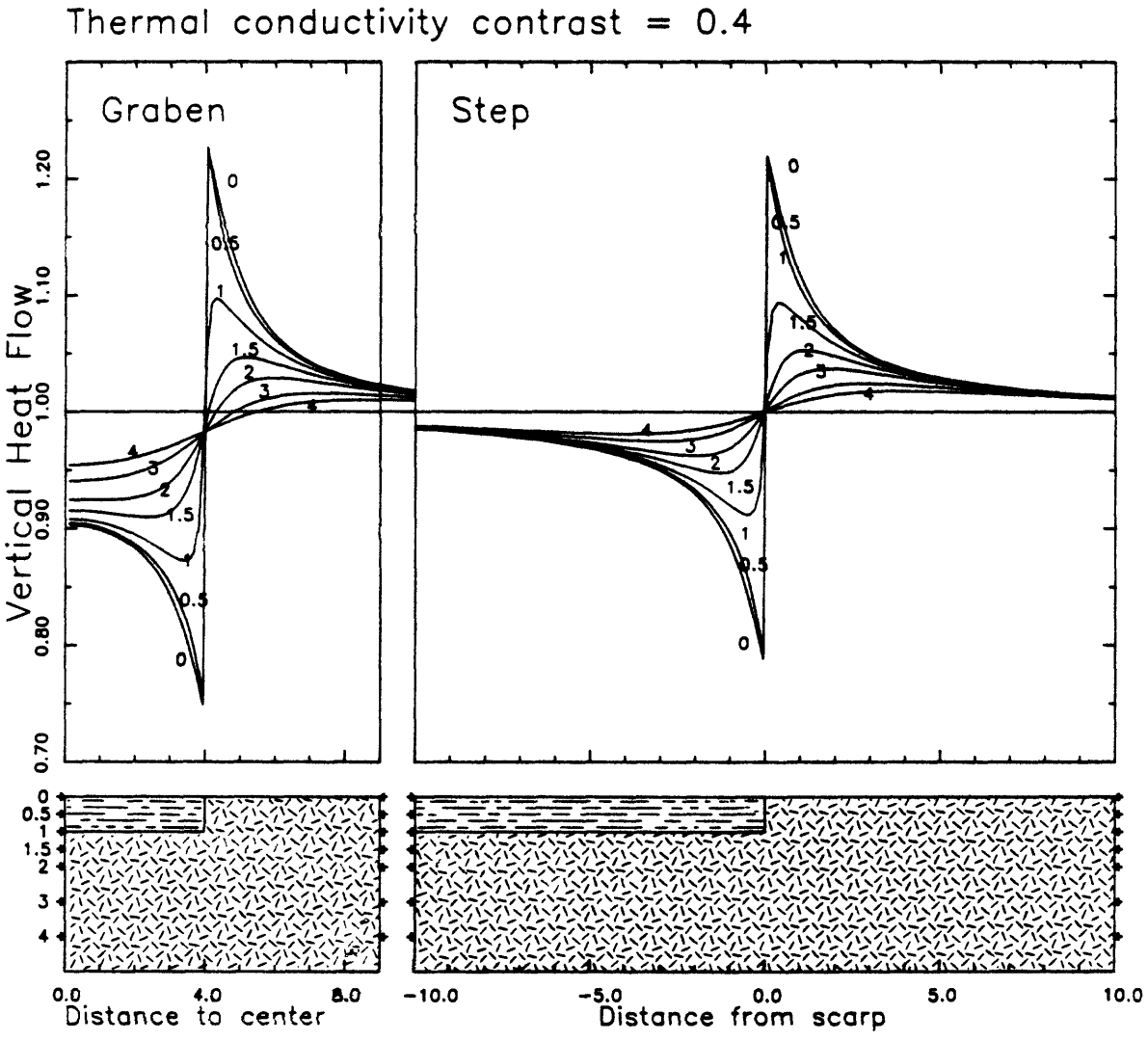

Figure 3: The variation of vertical heat flow with depth over two models juxtaposing material of moderate difference in thermal conductivity at a steep surface contact. Each heat flow curve is labeled with its calculation depth, normalized to scarp height. The lower blocks of the figure depict the model geometry. Small arrows mark the depths where heat flow is calculated. The stippled region has low thermal conductivity compared with the rest of the model. All distances are normalized to a unit scarp height.

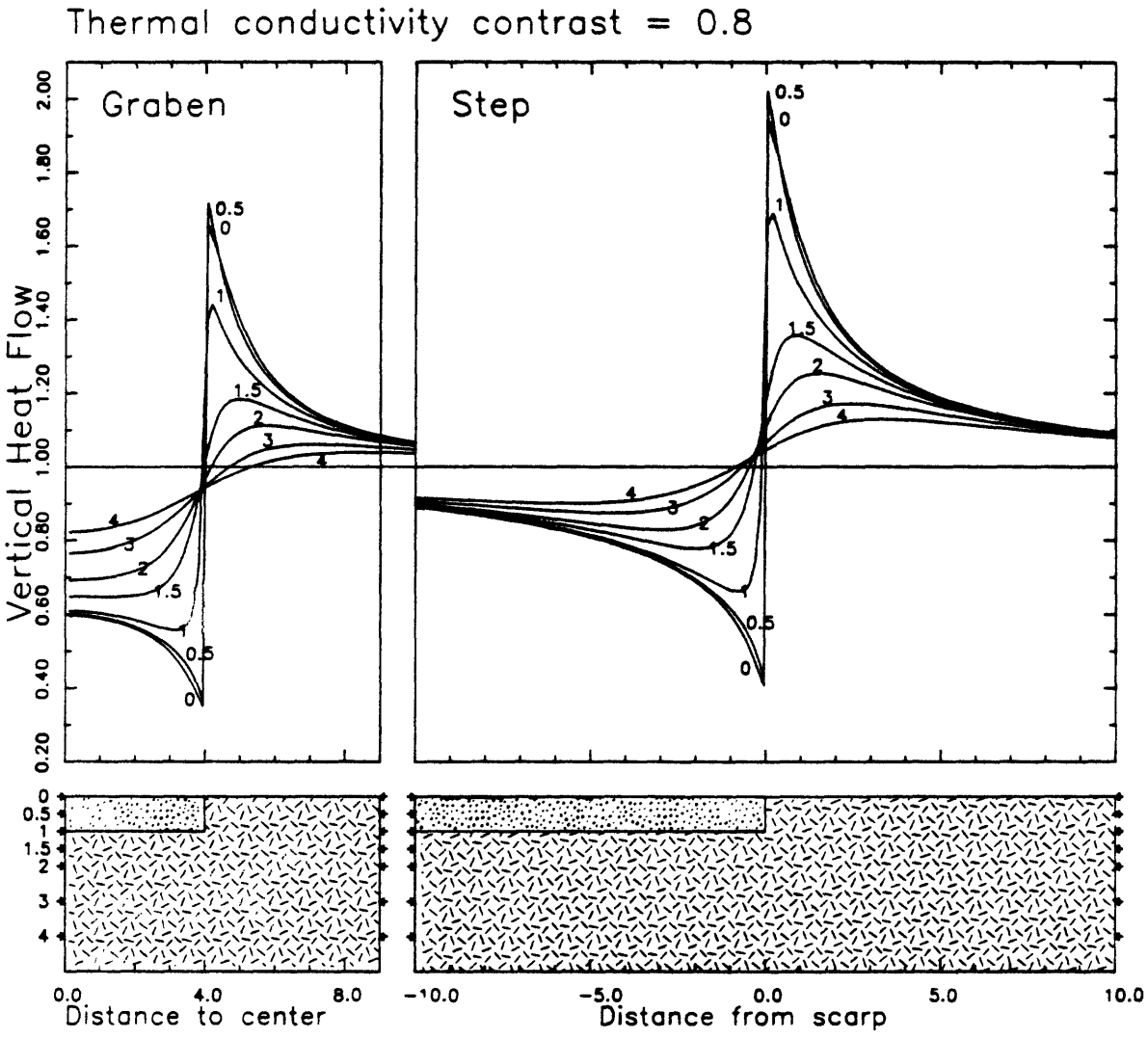

Figure 4: The variation of vertical heat flow with depth over two models juxtaposing material of large difference in thermal conductivity at a steep surface contact. Each heat flow curve is labeled with its calculation depth, normalized to scarp height. The lower blocks of the figure depict the model geometry. Small arrows mark the depths where heat flow is calculated. The stippled region has low thermal conductivity compared with the rest of the model. All distances are normalized to a unit scarp height.

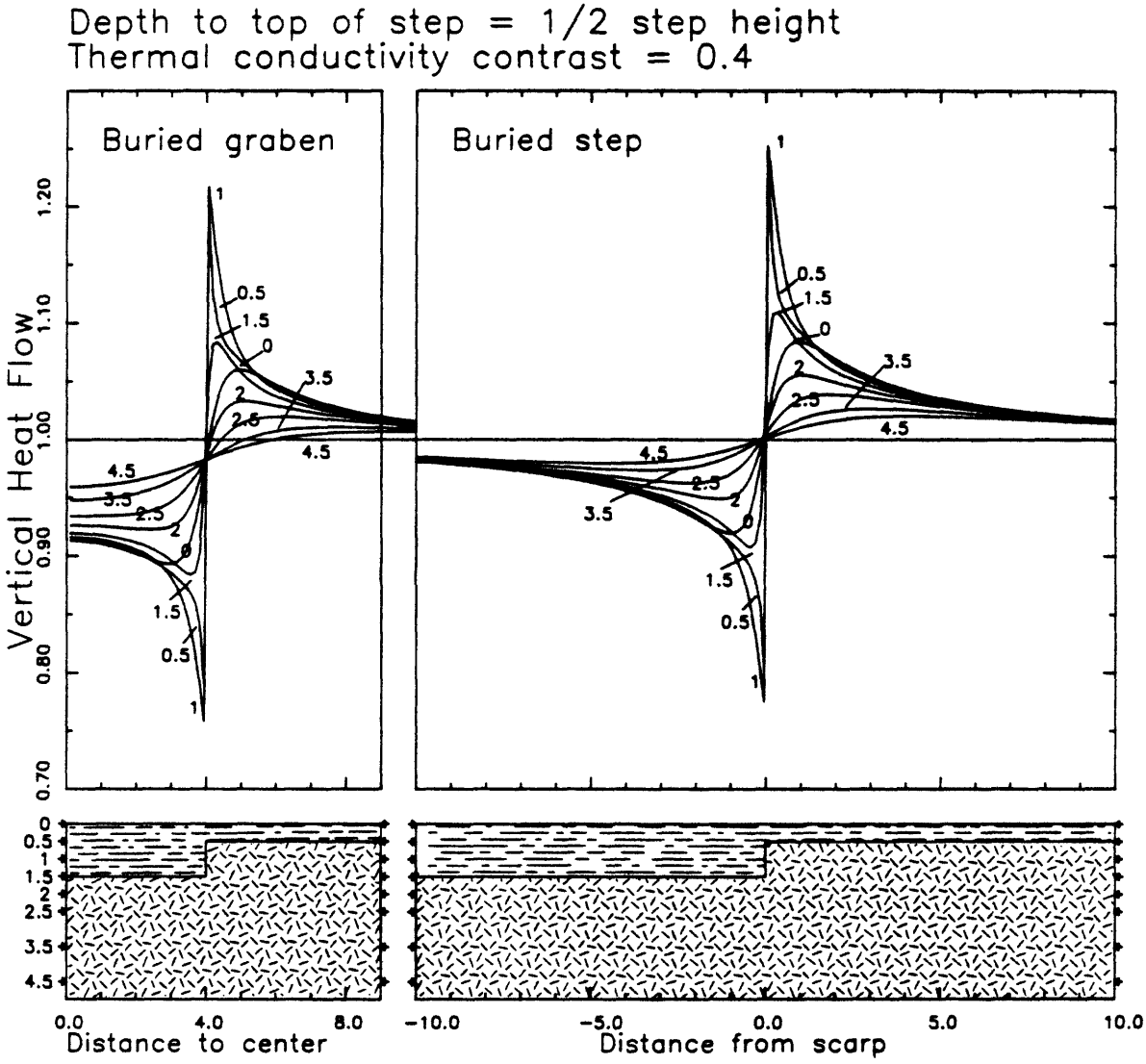

Figure 5: The variation of vertical heat flow with depth over two models juxtaposing material of moderate difference in thermal conductivity at a steep buried contact. Each heat flow curve is labeled with its calculation depth, normalized to scarp height. The lower blocks of the figure depict the model geometry. Small arrows mark the depths where heat flow is calculated. The stippled region has low thermal conductivity compared with the rest of the model. All distances are normalized to a unit scarp height.

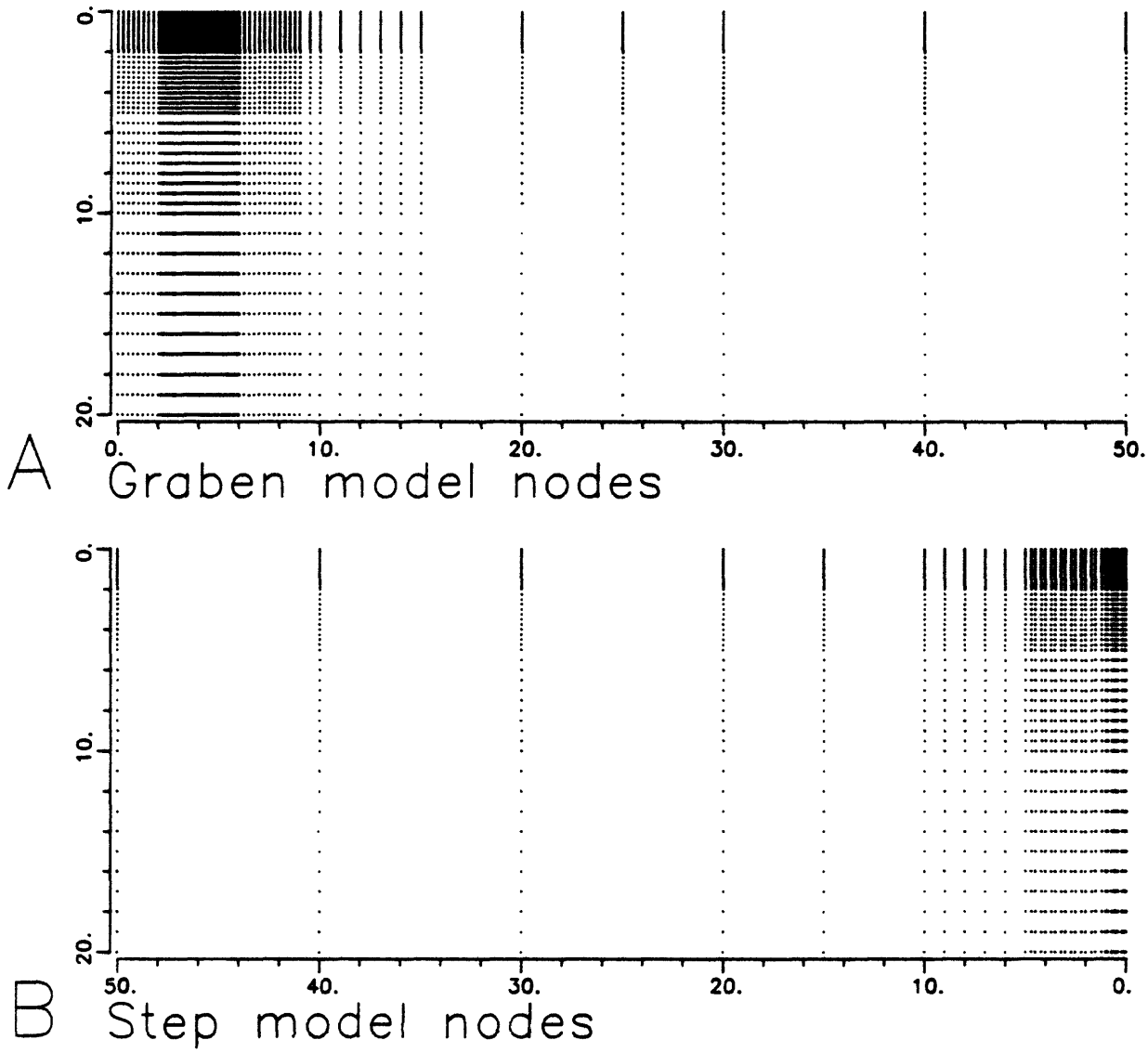

Figure 6: The node geometry of the finite element models. A depicts the entire graben model. B depicts half of the symmetric step model. The nodes are closely spaced in the regions of the model where heat flow varies the most.